Supplemental materials

Expanded Materials and Methods

Plasmid construction and transfection

Wild type human adiponectin receptor 1 (hAdipoR1^{WT}) cDNA were subcloned in-frame into the 3XFlag plasmid vector using convenient restriction sites HindIII and Xbal. To identify the specific site responsible for phosphorylative desensitization, Ser^{7}, Thr^{24}, Ser^{201} and Ser^{205} were individually or all mutated to alanine via an In-Fusion HD cloning kit (Takara, 63965) per manufacturer protocol. Additionally, Ser^{205} was mutated to glutamic acid to produce a pseudo-phosphorylation mutation. Primers used for each mutation were as follows:

Mutations	Forward primers (5'-3')	Reverse primers (5'-3')
Serine 7 to alanine (S7A)	ACAAAGGAGCTGTGGT GGCACAGGGGA	CCACAGCTCCTTTGTGGG AAGACATTCAGA
Threonine 24 to alanine (T24A)	AAGCTGACGCGGTGGA ACTGGCTGAACTG	CCACCGCGTCAGCTTCCC TGTTACTGGC
Serine 201 to alanine (S201A)	AGAAAGTCGCTCGGAC TTTTGCCAAACTGG	TCCGAGCGACTTTCTCTG AATGACAATAGACG
Serine 205 to alanine (S205A)	GGACTTTTGCCAAACTG GACTATTCAGGGATTGC	GTTTGGCAAAAGTCCGAG AGACTTTCTCTG
Serine 205 to glutamic acid (S205E)	GACTTTTGAGAAACTG GACTATTCAGGGATTGC TC	AGTTTCTCAAAAGTCCGA GAGACTTTCTCTG

Plasmids were mixed with Superfect Transfection Reagent (Qiagen, 301307) and administered to cells for 4 hours per manufacturer protocol. Medium was then changed to complete culture media sans antibiotics. 24 hours after plasmid transfection, the cells were infected with GRK2 adenovirus. After an additional 48 hours, cells were treated with APN (2 μg/mL) for 30 minutes.

Adeno-associated virus 9 (AAV9) vector production

The AAV9-cTNT-eGFP plasmid, AAV helper plasmid pAdDeltaF6, and AAV packaging plasmid pAAV2/9n used for producing AAV9-eGFP vector were purchased from the Penn Vector Core at the University of Pennsylvania. All plasmids were amplified in Stbl2 cells and purified with Qiagen EndoFree plasmid Maxi kits. 293T/17 cells were transfected with these three kinds of

plasmids concomitantly via PEI method for viral packaging. For a 15 cm diameter dish preparation, 7μg AAV9-cTNT-eGFP plasmids, 20μg pAdDeltaF6 plasmids, 7μg pAAV2/9n plasmids, and 88μg PEI were mixed to form DNA-PEI precipitate, and added to 293T/17 cells. 60 hours later, cells were harvested in lysis buffer, treated with 10% sodium deoxycholate and benzonase, and subjected to 3 cycles of freeze/thaw. AAV9-eGFP virus in supernatant was purified thereafter by iodixanol gradient centrifugation. Virus as well as iodixanol was added to an Amicon Ultra-15 100k MWCO centration unit for dialysis.

To produce AAV9-hAdipoR1^{WT}, AAV9-hAdipoR1^{S205A}, and AAV9-hAdipoR1^{S205E} vectors, the eGFP sequence from AAV9-cTNT-eGFP plasmid was replaced by hAdipoR1^{WT}, hAdipoR1^{S205A}, and hAdipoR1^{S205E} respectively, as follows. Primers used for PCR were: 5'-ATAGGCTAGCATGTCTTCCCACAAAGGATCTGTG-3'(forward), 5'-TCTAGGTACCTCAGAGAAGGGTGTCATC-3'(reverse). After the AAV9-cTNT-eGFP plasmid was digested by NheI and KPNI enzymes, the above PCR products were added for ligation by Takara ligation kit per manufacturer protocol. Final plasmids were amplified in stbl2 cells and verified via enzyme digestion using NheI and KPNI. Virus was packaged and purified as stated above.

The titer of the AAV9 vector (viral genomes/ml) was determined by quantitative real-time PCR. Firstly, virus was prepared by adding 45μl DNAse solution to 5 μl virus to remove residual plasmid DNA from purification, followed by 50μl proteinase K solution. 1μl virus preparation solution was used for quantitative real-time PCR. The following primers were used for amplifying hAdipoR1 (WT, S205A, or S205E): 5'-ATAGGCTAGCATGTCTTCCCACAAAGGATCTGTG-3'(forward), 5'-CAGACCTTGTACACAAACTCTTCCATCTTCTCCA-3'(reverse). Known copy numbers of AdipoR1 PCR fragments were used to construct standard curves for quantification.

Echocardiography

Echocardiography was conducted before coronary occlusion (control) and weekly after MI. Mice were anesthetized with 3% isoflurane. Transthoracic echocardiography was performed using a Vevo 2100 ultrasound system (VisualSonics, Canada) with a 30 MHz linear transducer. Images were acquired in the short-axis M-mode at the level of the papillary muscles. Left ventricular ejection fraction (LVEF) and left ventricular fraction shortening (LVFS) were calculated by computer algorithms. Long-axis B-mode images were recorded for longitudinal and radial speckle-tracking strain analysis via VevoStrain software (VisualSonics, Canada), as previously described[51,

[52]. All measurements were determined by a single blinded echocardiographer.

Neonatal mouse ventricular myocyte (NMVMs) isolation

Primary cultures of NMVMs from 1-2 day-old AdipoR1-KO mouse pups were prepared per previously described method[22,53] with slight modification. Briefly, after euthanasia of mouse pups, hearts were removed, ventricles were minced, and myocytes were isolated with 1.0 mg/mL collagenase type II (ThermoFisher scientific, 17101015). Isolated myocytes were collected at 10 minute intervals for 3 cycles. Cells were re-suspended in high glucose DMEM (Sigma-Aldrich, D5796) containing 10% FBS, 10mM HEPES, and 0.1 mM 5-Bromo-2'-deoxyuridine (BrdU, Sigma-Aldrich, B5002), and plated in culture dishes for 90 minutes to allow fast-adherent fibroblast attachment. Non-adherent cells (ventricular myocytes) were collected and plated in 6-well plates or Millicell EZ SLIDE 8 well glass plates. The medium was replaced the following day with M199 containing 0.5% FBS and 10mM HEPES.

Adult cardiomyocyte isolation

8-10 week-old adult AdipoR1-KO mice with cardiomyocyte-specific over-expression of hAdipoR1^{WT} (AdipoR1-KO/AAV9-hAdipoR1^{WT}) or hAdipoR1^{S205A} (AdipoR1-KO/AAV9-hAdipoR1^{S205A}) were sacrificed. Cardiomyocytes were isolated as previously described[54] with minor modification. In brief, descending aorta and inferior vena cava were harvested. EDTA buffer was injected into the right ventricle. The ascending aorta was cut. The heart was removed and subjected to perfusion and collagenase buffer injection. Left ventricle was cut into pieces, gently teased and filtered. Adult cardiomyocytes were collected in stop buffer. 5 uM $CaCl_2$ was added to the cells every 8 minutes five times. Cardiomyocytes were resuspended in plating medium upon Millicell EZ SLIDE 8 well glass pre-coated with 5 ug/ml laminin (ThermoFisher Scientific, 23017015) in PBS. 2 hours later, plating medium was replaced by culture medium. To extend adult cardiomyocyte survival in culture for virus infection, 20uM blebbistatin (Sigma-Aldrich, B0560) was added to culture medium as recently reported[55,56].

Adenoviral Infection

NMVMs or adult cardiomyocytes were infected with adenoviral vectors containing cDNAs for GRK2 (Ad-GRK2) using a multiplicity of infection of 1000 viral particles per cell (20 infectious units per well). The efficiency of adenoviral gene transfer was monitored 12, 24, 48, and 72 hours later by Western blot. Cells infected with adenovirus containing empty vectors (Ad-Empty) served as control.

Cell viability assay

Cell viability was determined via MTT [3-(4,5-dimethythiazol-2-yl) 2,5-diphenyltetrazolium bromide] assay per previous study[57]. Briefly, 24 hours after being transfected with 3XFlag-hAdipoR1^{WT} or hAdipoR1^{S205A}, NMVMs isolated from AdipoR1-KO mice were transfected with either empty or Ad-GRK2 vector. 48 hours later, cells were treated with APN (2 μg/mL) for 24 hours followed by H_2O_2 for 2 hours. MTT solution was then added to the cells (final concentration 0.5 mg/ml) for 4 hours. The medium was carefully removed and 100 μl DMSO was added to each well. The absorbance values at 570 nm were read by a multi-well spectrophotometer SpectraMax M5 (Molecular Devices).

Lactate dehydrogenase (LDH) release assay

LDH release was detected by LDH Cytotoxicity Detection kit (Takara, MK401) per manufacturer protocol. After treatments, the NMVMs were incubated with H_2O_2 for 2 hours. Cell medium was harvested and centrifuged at 250 × g for 10 minutes. 100 μl supernatant was mixed with an equal volume of pre-prepared solution (catalyst/dye buffer ratio=1:45) for 30 minutes at room temperature. The absorbance values at 490 nm were read by a multi-well spectrophotometer SpectraMax M5 (Molecular Devices).

Western blot

Proteins were extracted from tissues or cells using cell lysis buffer (10×) (CST, 9803) supplemented with a protease inhibitor cocktail (ThermoFisher Scientific, 78438). Equivalent amounts of proteins (50~70 μg) were separated on 4-20% gradient SDS-PAGE gel, transferred onto a PVDF membrane and blocked with 5% skim milk. The membranes were incubated with primary antibodies overnight at 4°C, then incubated with secondary HRP-conjugated anti-mouse antibody (CST, #7076) or anti-rabbit antibody (CST, #7074) at room temperature for 2 hours. The bands were visualized and analyzed by use of an enhanced chemiluminescent (ECL) detection system (Image Lab, Bio-Rad). The primary antibodies used were: anti-phospho-ERK1/2 rabbit monoclonal antibody (Cell Signaling Technology, #4370), anti-ERK1/2 rabbit monoclonal antibody (CST, #4695), anti-phospho-AMPKα rabbit antibody (CST, #2531), anti-AMPKα rabbit antibody (CST, #2603), anti-phospho-ACC rabbit monoclonal antibody (CST, #11818), anti-ACC rabbit antibody (CST, #3662), anti-cleaved caspase-3 rabbit polyclonal antibody (CST #9661), anti-caspase-3 rabbit polyclonal antibody (CST, #9662), anti-phospho-AP2M1 rabbit monoclonal antibody (CST, #7399), anti-AP2M1 rabbit monoclonal antibody (Abcam #ab75995), anti-GRK2

rabbit antibody (CST, #3982s), anti-adipoR1 mouse monoclonal antibody (Santa Cruz Biotechnology, sc-518030), Anti-β-arrestin1/2 rabbit monoclonal antibody (CST, #4674), anti-GFP rabbit polyclonal antibody (Genscript, A01704), anti-β-actin mouse monoclonal antibody (Santa Cruz Biotechnology, sc-47778), and anti-GAPDH rabbit monoclonal antibody (CST, #2118).

Coimmunoprecipitation (Co-IP)

NMVMs were transfected with 3XFlag-hAdipoR1^{WT}. 24 hours later, cells were infected with Ad-GRK2 for 48 hours. Cells were washed once with PBS, and lysed with cold 1×lysis buffer (CST, #9803) supplemented with a protease inhibitor cocktail (ThermoFisher Scientific, 78438). Cell lysates were then incubated with anti-flag M2 (Sigma-Aldrich, F1804) rabbit antibody and supplemented with protein A plus ultralink resin (ThermoFisher Scientific, 53142) and rocked overnight (4°C). The protein A beads were washed extensively with lysis buffer. Proteins were eluted from the beads and resolved by IgG elusion buffer (ThermoFisher Scientific, 1856202). Samples were heated and separated by electrophoresis. After transfer to polyvinylidene fluoride membranes, proteins were immunoblotted with anti-β-arrestin1/2 antibody (CST, #4674) as described above.

Quantitative PCR

RNA from NMVMs was extracted via a TRIzol reagent (ThermoFisher Scientific, 15596026), and cDNA was prepared from 1 μg RNA with SuperScript III First-Strand Synthesis System (ThermoFisher Scientific, 18080051) per manufacturer protocol. PCR was then performed with SYBR Green PCR Master mix (ThermoFisher Scientific, 4344463) in a Real-Time PCR machine (Applied Biosystems). Primers were purchased from Integrated DNA Technologies. Actb (β-actin) RNA served as housekeeping targets. AdipoR1 primers used were: 5'-TCGGACTTTTTCCAAACTGGAC-3' (forward) and 5'-TTGACAAAGCCCTCAGCGAT-3' (reverse). Final data were normalized by the standard comparative cycle threshold method.

Assessment of endocytosis via the SNAP-Surface method

SNAP-Surface system is an established method utilized in membrane protein internalization investigation. The hAdipoR1^{WT} and hAdipoR1^{S205A} were cloned into the pSNAP$_f$ vector (NEB #E9120S) for expression of fusion proteins with a C-terminal SNAP tag. Briefly, the following primers were used for PCR to amplify hAdipoR1^{WT} and hAdipoR1^{S205A}: 5'-ATAGGCTAGCGCCACCATGTCTTCCCACAAAGGATCTGTGGTG -3'(forward), 5'-

TTGGCGCGCCGAGAAGGGTGTCATCAGTACAGCC -3'(reverse). The PCR products and $pSNAP_f$ vector were ligated by Takara ligation kit after digestion by NheI and AscI enzymes to form pSNAPf-hAdipoR1^{WT} and pSNAPf-hAdipoR1^{S205A} plasmids. The plasmids were then transfected into NMVMs isolated from AdipoR1-KO mice. After 72 hours, SNAP fluorescence labelling was used per manufacturer protocol (New England Biolabs). Briefly, the NMVMs were incubated with 5 μM cell-impermeable SNAP-Surface 549 fluorescent substrate at 37℃ for 30 minutes to make fusion proteins visible, and cells were washed 3 times with PBS. The images were acquired by Olympus BX51 fluorescence microscopy. All measurements were determined by a single blinded research fellow.

Immunofluorescent staining and colocalization analysis

Cultured adult cardiomyocytes expressing hAdipoR1^{WT} or hAdipoR1^{S205A} were fixed with 2% formaldehyde for 20 minutes and permeabilized with methanol for 10 minutes followed by 0.5% casein incubation. Cardiomyocytes were then incubated with mouse anti-AdipoR1 (Santa Cruz, sc-518030, 1:100) and rabbit anti-Rab5 (Cell Signaling Technology, #3547, 1:200) or mouse anti-AdipoR1 and rabbit anti-LAMP2 (Bioss, BS-2379R, 1:100) at 4 ℃ overnight. Cells were washed and incubated with an anti-mouse secondary antibody labeled with Alexa Fluor 546 (ThermoFisher Scientific, A-11003) and anti-rabbit secondary antibody labeled with Cy5 (Abcam, Ab6564) at room temperature for 1 hour. Adult cardiomyocytes expressing hAdipoR1^{WT} were probed with secondary antibodies, without primary, as negative controls to distinguish genuine target staining from background. Images were taken by NIKON Eclipse Ti2 confocal microscopy, and analyzed for colocalization by using Fiji software[58]. All measurements were determined by a single blinded research fellow.

Masson's trichrome staining

Masson's trichrome staining evaluated cardiac interstitial fibrosis[59]. Coronal sections (5 μm thick) were prepared for Masson's trichrome staining per manufacturer protocol (Sigma-Aldrich, HT15). Fibrosis was measured via Olympus cellSens Microscope Imaging Software, and calculated by Fibrosis Area/LV Area (Fiji software). All measurements were determined by a single blinded research fellow.

Online Figures

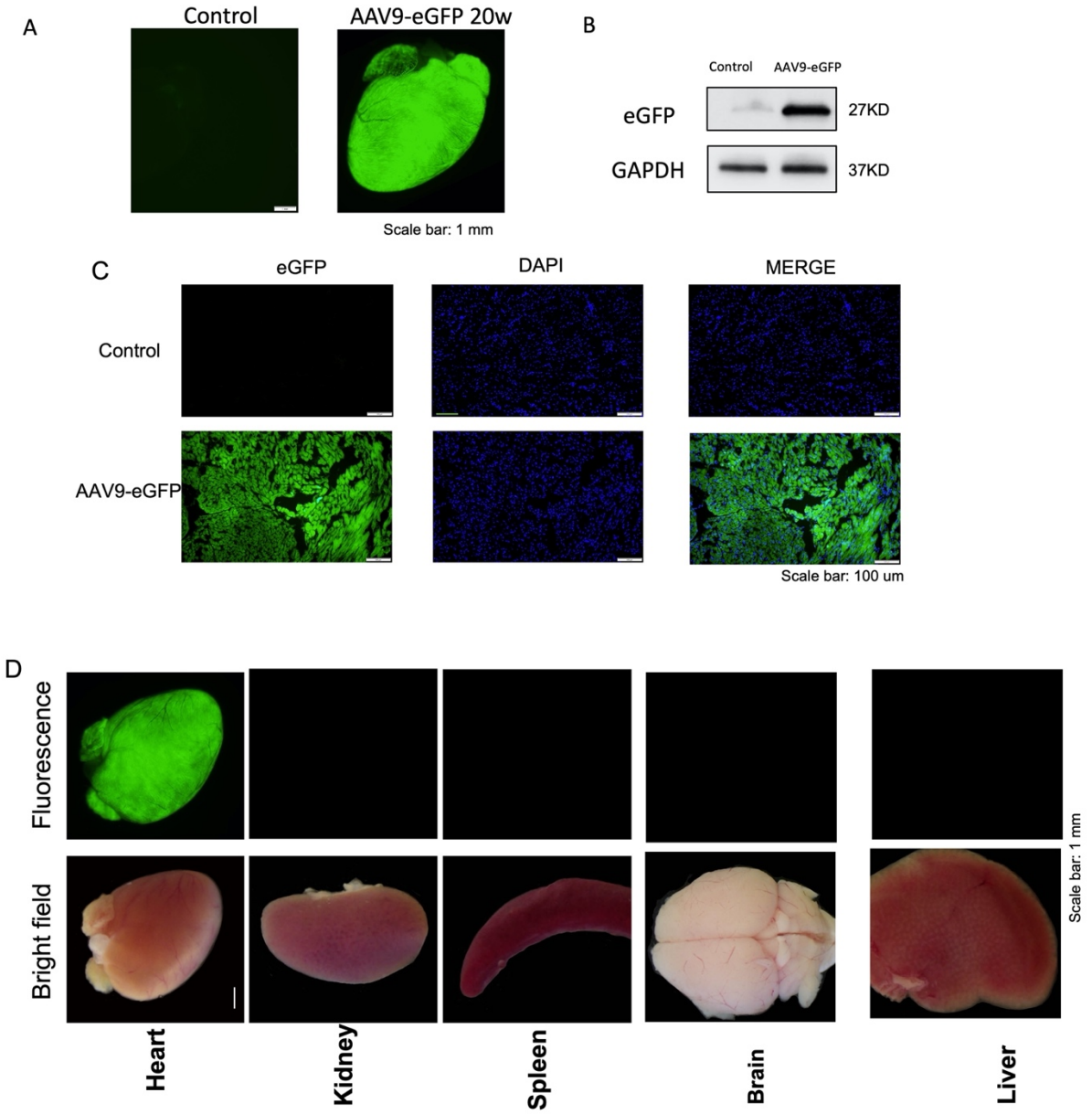

Figure S1. AdipoR1-KO mice injected with AAV9-cTNT-eGFP revealed heart-specific expression of eGFP. A/C/D. Hearts, not other organs expresses eGFP 20 weeks after AAV9 injection. B. Western blots shows expression of eGFP in hearts from AAV9-cTNT-eGFP-treated mice.

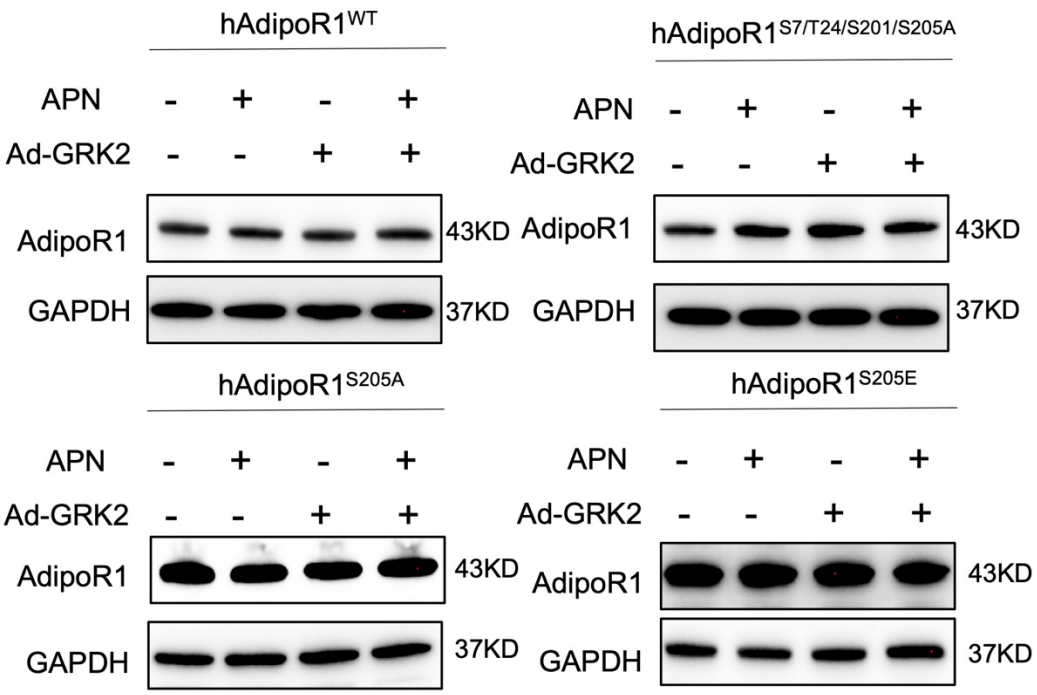

Figure S2. AdipoR1 expression 24 hours after GRK2 expression, confirming comparable overexpression of exogenous constructs.

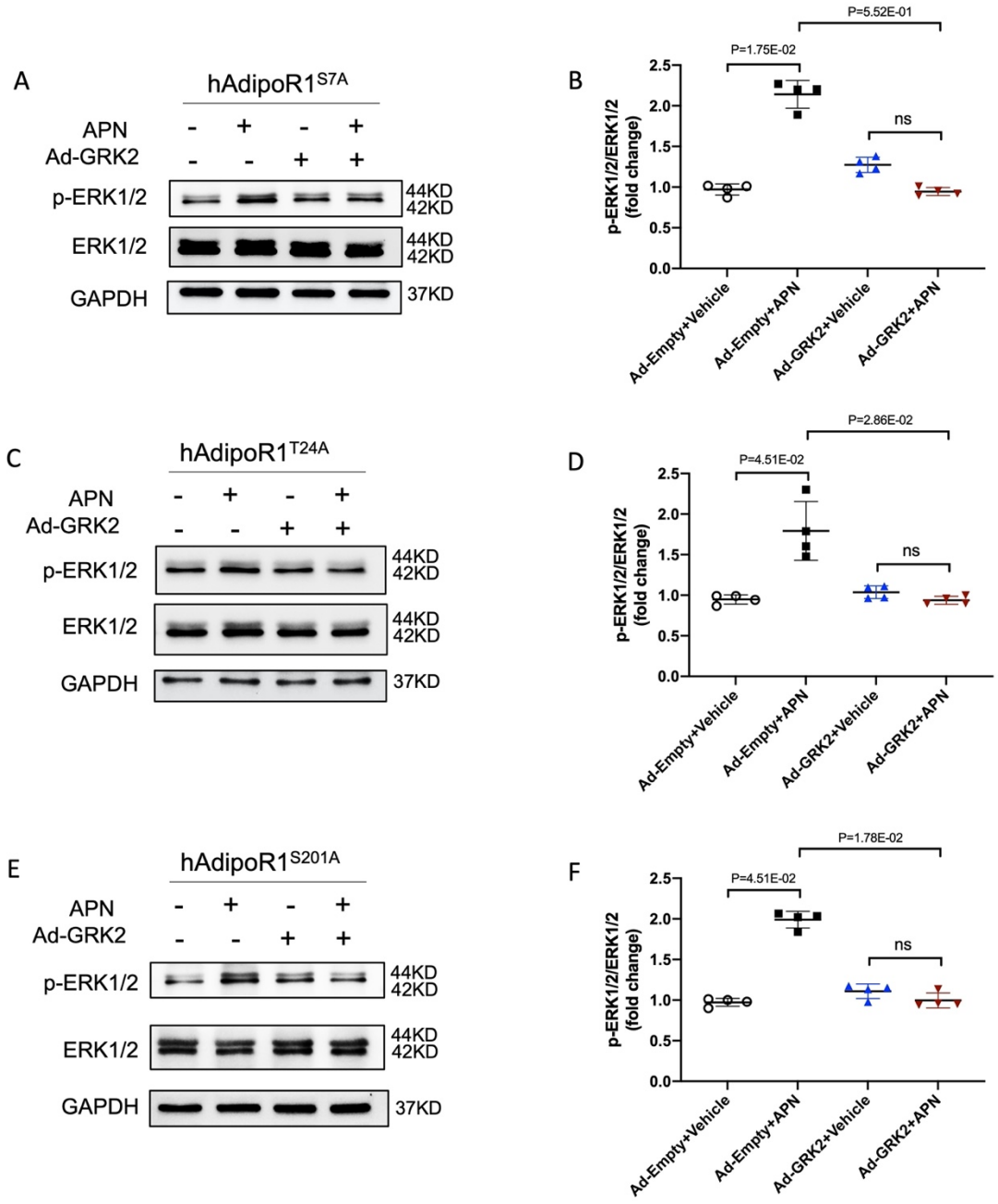

Figure S3. A/C/E: Effect of APN on p-ERK1/2 activation in AdipoR1-KO/hAdipoR1^{S7A}, AdipoR1-KO/hAdipoR1^{T24A} or AdipoR1-KO/hAdipoR1^{S201A} cardiomyocytes.
B/D/F: Quantification of the western blot results (n = 4). Statistical significance was evaluated by a Kruskal-Wallis test. Post hoc pairwise tests for indicated group pairs were performed after Dunn correction. Ns indicates not significant.

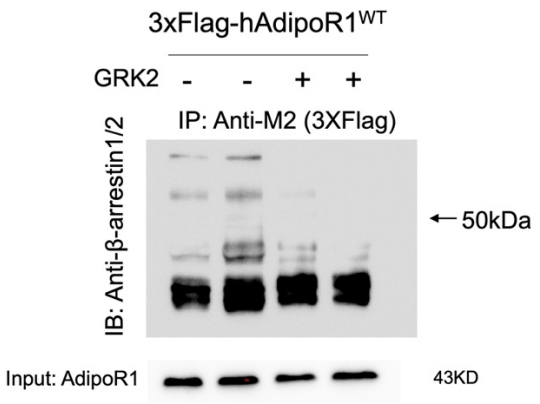

Figure S4. Co-immunoprecipitation (Co-IP) and immunoblot (IB) analysis of 3XFLAG-adipoR1 with β-arrestin1/2 in NMVMs under stimulation of APN (24 hours after GRK2OE).

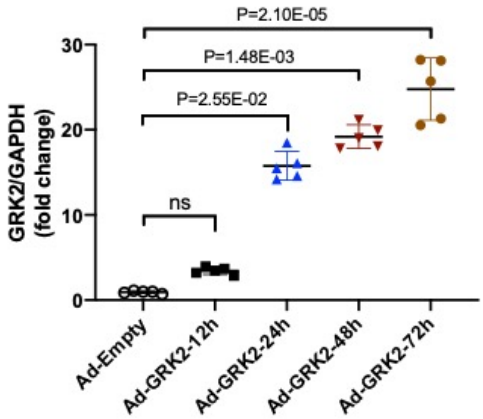

Figure S5. Quantification of the western blot of GRK2 expression normalized to GAPDH in hAdipoR1WT over-expressed NMVMs infected with adenovirus (n = 5). Statistical significance was evaluated by a Kruskal-Wallis test. Post hoc pairwise tests for indicated group pairs were performed after Dunn correction. Ns indicates not significant.

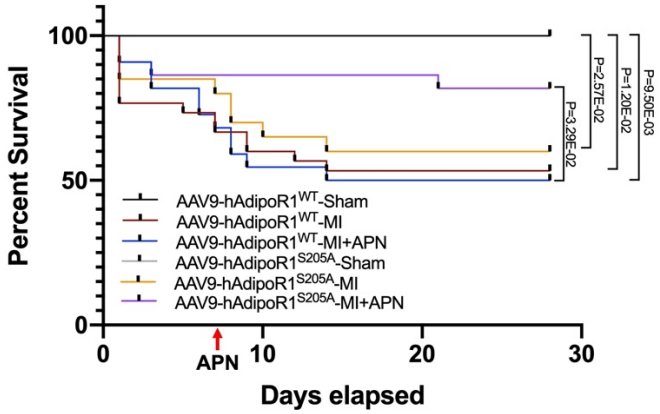

Figure S6. Administration of APN 7 days after MI failed to improve survival rate in AAV9-hAdipoR1^{WT} mice. In contrast, administration of APN 7 days after MI significantly improved survival rate in AAV9-hAdipoR1^{205A} mice. Survival curve analysis was made by a log-rank test (n=10 for AAV9-hAdipoR1^{WT}-Sham, n=30 for AAV9-hAdipoR1^{WT}-MI, n=22 for AAV9-hAdipoR1^{WT}-MI+APN, n=10 for AAV9-hAdipoR1^{S205A}-Sham, n=20 for AAV9-hAdipoR1^{S205A}-MI, n=22 for AAV9-hAdipoR1^{S205A}-MI+APN group).

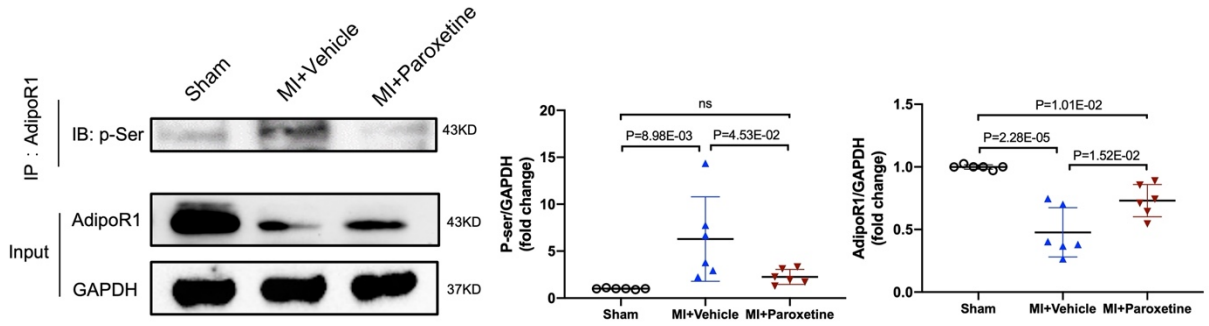

Figure S7. Paroxetine treatment significantly attenuated AdipoR1 phosphorylation and preserved AdipoR1 expression level in MI heart. N=6.

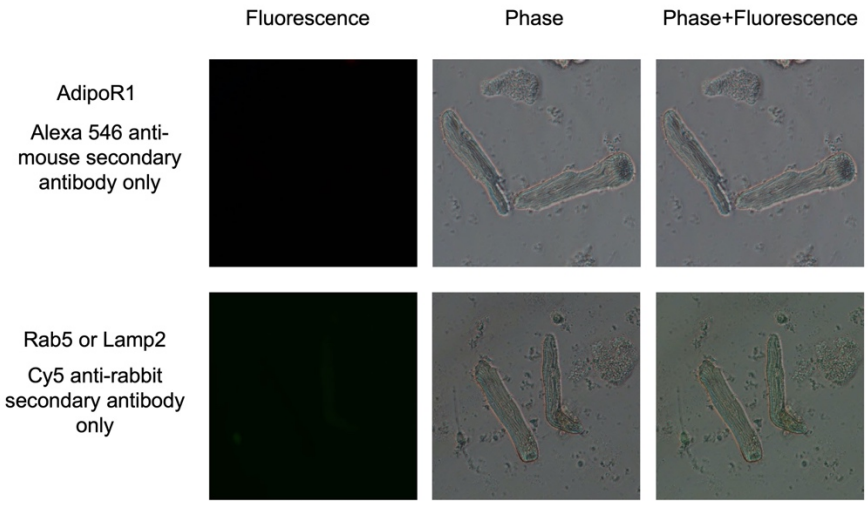

Figure S8. Negative controls for immunocytochemistry. Representative secondary antibody-only control images in adult cardiomyocytes for AdipoR1 and Rab5 or Lamp2 colocalization experiments, as negative controls for Figure 3D and Figure 6A.

Online Tables

Table S1 Cardiac function of AdipoR1-KO/AAV9-hAdipoR1^{WT} mice by echocardiography

Treatment groups	EF (%)	FS (%)	Radial Strain (%)	Radial Strain Rate (1/s)	Longitudinal Strain (%)	Longitudinal Strain Rate (1/s)
Before MI						
Sham	61.50±8.14	34.97±4.30	51.62±6.70	11.93±2.12	-21.88±3.05	-11.14±2.24
MI	63.71±5.75	36.00±4.44	53.07±5.44	10.73±2.08	-21.92±4.12	-11.32±2.05
MI+APN	63.17±6.26	36.32±4.63	53.22±5.50	10.60±2.26	-23.43±3.89	-10.63±1.83
1 week after MI						
Sham	57.83±5.15	35.00±3.86	56.03±5.35	12.51±2.02	-21.23±1.54	-10.88±2.11
MI	25.14±8.95**	14.48±3.75**	17.30±7.70**	7.40±0.73**	-12.66±4.88*	-6.78±2.61
MI+APN	25.33±6.99**	14.58±2.19**	19.41±7.25**	8.58±2.10*	-11.99±3.96**	-6.92±2.60
2 weeks after MI						
Sham	60.83±7.99	36.23±4.12	55.18±7.13	11.21±1.19	-24.72±4.75	-11.55±1.96
MI	17.17±4.63**	14.95±5.44**	14.80±5.21**	5.75±1.14**	-9.35±1.83**	-6.08±2.06**
MI+APN	18.50±4.35**	14.93±6.07**	15.63±3.56**	5.72±1.20**	-9.50±2.49**	-6.55±1.68**
3 weeks after MI						
Sham	61.33±6.99	35.42±4.00	56.43±4.92	11.76±1.83	-24.53±3.99	-10.85±1.52
MI	15.33±5.00**	13.03±2.40**	12.38±6.21**	6.12±1.22**	-7.42±2.20**	-5.82±2.21**
MI+APN	17.12±5.46**	14.37±5.64**	13.90±5.82**	6.65±0.96**	-8.10±2.55**	-5.73±2.03**
4 weeks after MI						
Sham	59.50±6.26	35.13±5.04	54.77±5.25	12.39±2.21	-22.18±2.29	-11.27±1.89
MI	14.17±3.62**	13.17±2.46**	11.42±3.52**	6.53±1.30**	-6.73±1.96**	-5.12±1.32**
MI+APN	15.83±2.91**	11.35±2.63**	13.72±4.42**	7.15±1.01**	-7.43±3.43**	-5.60±1.85**

$^{**}p<0.01$, $^{*}p<0.05$ vs. Sham; $^{\#\#}p<0.01$, $^{\#}p<0.05$ vs. MI.

Table S2 Cardiac function of AdipoR1-KO/AAV9-hAdipoR1^{S205A} mice by echocardiography

Treatment groups	EF (%)	FS (%)	Radial Strain (%)	Radial Strain Rate (1/s)	Longitudinal Strain (%)	Longitudinal Strain Rate (1/s)
Before MI						
Sham	62.17±5.20	35.50±4.36	52.75±8.00	11.04±1.90	-24.33±3.50	-9.67±1.62
MI	61.26±5.56	34.68±4.02	48.14±3.35	10.70±1.48	-23.17±3.58	-9.98±1.22
MI+APN	60.58±6.88	31.71±3.08	52.50±7.29	11.27±1.86	-21.09±7.65	-10.00±1.02
1 week after MI						
Sham	61.10±7.61	32.82±4.18	51.55±6.27	10.86±1.61	-21.26±2.94	-10.03±1.56
MI	30.12±7.24**	16.01±3.88**	17.96±1.46**	5.77±1.90*	-4.71±3.58**	-3.36±0.95**
MI+APN	25.67±8.69**	14.13±3.62**	18.39±2.90**	5.70±2.58*	-5.44±1.71**	-3.19±1.02**
2 weeks after MI						
Sham	65.17±8.45	34.5±3.82	53.37±6.40	11.79±1.19	-21.10±1.36	-8.78±1.12
MI	25.00±7.48**	15.22±3.73**	16.44±4.71**	6.56±1.71**	-5.14±2.01**	-3.39±1.43**
MI+APN	35.13±6.17**	20.35±6.33*	26.76±5.48**	7.69±2.06*	-10.00±3.80**	-5.60±1.42*
3 weeks after MI						
Sham	59.44±5.32	33.67±5.57	48.47±5.66	10.90±1.27	-22.10±2.54	-9.86±1.67
MI	18.29±4.98**	11.06±2.89**	17.42±2.55**	5.00±1.79**	-5.57±2.63**	-3.10±1.61**
MI+APN	31.85±7.26$^{**,\#\#}$	20.84±4.91$^{*,\#}$	27.83± 5.92$^{**,\#}$	8.18±1.90$^{*,\#}$	-12.17±5.84$^{*,\#}$	-7.09±1.28$^{*,\#}$
4 weeks after MI						
Sham	57.83±7.26	34.00±3.74	54.37±5.99	11.98±1.43	-21.40±2.74	-9.74±1.35
MI	17.94±6.00**	14.40±1.85**	12.60±3.22**	5.32±1.60**	-5.85±4.21**	-2.75±0.51**
MI+APN	35.79±4.72$^{**,\#\#}$	23.91±1.71$^{**,\#\#}$	24.72± 7.33$^{**,\#}$	8.36±1.43$^{*,\#}$	-13.14±4.10$^{**,\#}$	-7.27±0.95$^{*,\#\#}$

$^{**}p<0.01$, $^{*}p<0.05$ vs. Sham; $^{\#\#}p<0.01$, $^{\#}p<0.05$ vs. MI.

Table S3 Cardiac function of AdipoR1-KO/AAV9-control mice by echocardiography

Group	EF (%)	FS (%)	Radial Strain (%)	Radial Strain Rate (1/s)	Longitudinal Strain (%)	Longitudinal Strain Rate (1/s)
AdipoR1-KO/AAV9-control	69.06±4.13	36.00±3.36	56.12±10.09	12.41±2.24	-23.95±4.67	-9.01±1.47

Table S4 Cardiac function of AdipoR1-KO/AAV9-hAdipoR1^{S205E} mice by echocardiography

Group	EF (%)	FS (%)	Radial Strain (%)	Radial Strain Rate (1/s)	Longitudinal Strain (%)	Longitudinal Strain Rate (1/s)
AdipoR1-KO/AAV9-hAdipoR1^{S205E}	62.50±5.50	35.23±3.15	54.68±6.55	12.63±2.90	-22.92±3.20	-9.57±1.81

Table S5 Supporting Statistical Information

Figure	Pairwise Comparison	Shapiro-Wilk for normality	Statistical Test	Raw P value	Multiple comparisons	Corrected P value
Figure 1B						
p-ERK1/2/ERK1/2		Not normal	Kruskal-Wallis	1.85E-3	Dunn's	
	Ad-Empty+Vehicle vs. Ad-Empty+APN					1.09E-3
	Ad-GRK2+Vehicle vs. Ad-GRK2+APN					8.82E-1
	Ad-Empty+APN vs. Ad-GRK2+APN					4.50E-2
p-AMPK/AMPK		Not normal	Kruskal-Wallis	1.63E-2	Dunn's	
	Ad-Empty+Vehicle vs. Ad-Empty+APN					9.35E-3
	Ad-GRK2+Vehicle vs. Ad-GRK2+APN					7.10E-1
	Ad-Empty+APN vs. Ad-GRK2+APN					3.76E-2
p-ACC/ACC		Not normal	Kruskal-Wallis	7.85E-3	Dunn's	
	Ad-Empty+Vehicle vs. Ad-Empty+APN					7.51E-3
	Ad-GRK2+Vehicle vs. Ad-GRK2+APN					3.73E-1
	Ad-Empty+APN vs. Ad-GRK2+APN					7.47E-2
Figure 1D						
p-ERK1/2/ERK1/2		Not normal	Kruskal-Wallis	6.55E-4	Dunn's	
	Ad-Empty+Vehicle vs. Ad-Empty+APN					2.13E-2
	Ad-GRK2+Vehicle vs. Ad-GRK2+APN					1.43E-2
	Ad-Empty+APN vs. Ad-GRK2+APN					7.66E-1
p-AMPK/AMPK		Not normal	Kruskal-Wallis	1.99E-4	Dunn's	
	Ad-Empty+Vehicle vs. Ad-Empty+APN					1.43E-2
	Ad-GRK2+Vehicle vs. Ad-GRK2+APN					2.13E-2
	Ad-Empty+APN vs. Ad-GRK2+APN					4.58E-1
p-ACC/ACC		Not normal	Kruskal-Wallis	2.32E-4	Dunn's	
	Ad-Empty+Vehicle vs. Ad-Empty+APN					6.00E-3
	Ad-GRK2+Vehicle vs. Ad-GRK2+APN					4.50E-2
	Ad-Empty+APN vs. Ad-GRK2+APN					3.73E-1
Figure 1F						
p-ERK1/2/ERK1/2		Not normal	Kruskal-Wallis	4.06E-4	Dunn's	
	Ad-Empty+Vehicle vs. Ad-Empty+APN					2.13E-2
	Ad-GRK2+Vehicle vs. Ad-GRK2+APN					1.43E-2
	Ad-Empty+APN vs. Ad-GRK2+APN					6.56E-1
p-AMPK/AMPK		Not normal	Kruskal-Wallis	5.85E-4	Dunn's	
	Ad-Empty+Vehicle vs. Ad-Empty+APN					6.00E-3
	Ad-GRK2+Vehicle vs. Ad-GRK2+APN					4.50E-2
	Ad-Empty+APN vs. Ad-GRK2+APN					5.52E-2

p-ACC/ACC		Not normal	Kruskal-Wallis	9.58E-4	Dunn's	
	Ad-Empty+Vehicle vs. Ad-Empty+APN					1.16E-2
	Ad-GRK2+Vehicle vs. Ad-GRK2+APN					2.59E-2
	Ad-Empty+APN vs. Ad-GRK2+APN					7.66E-1
Figure 1H						
p-ERK1/2/ERK1/2		Not normal	Kruskal-Wallis	2.98E-1	N/A	
	Ad-Empty+Vehicle vs. Ad-Empty+APN					
	Ad-GRK2+Vehicle vs. Ad-GRK2+APN					
	Ad-Empty+APN vs. Ad-GRK2+APN					
p-AMPK/AMPK		Not normal	Kruskal-Wallis	3.14E-1	N/A	
	Ad-Empty+Vehicle vs. Ad-Empty+APN					
	Ad-GRK2+Vehicle vs. Ad-GRK2+APN					
	Ad-Empty+APN vs. Ad-GRK2+APN					
p-ACC/ACC		Not normal	Kruskal-Wallis	7.52E-1	N/A	
	Ad-Empty+Vehicle vs. Ad-Empty+APN					
	Ad-GRK2+Vehicle vs. Ad-GRK2+APN					
	Ad-Empty+APN vs. Ad-GRK2+APN					
Figure 2A						
Ad-Empty		Normal	One-way ANOVA	3.80E-20	Tukey's	
	Vehicle vs. H_2O_2					6.41E-11
	H_2O_2 vs. H_2O_2+APN					3.33E-03
	Vehicle vs. H_2O_2+APN					9.30E-09
Ad-GRK2		Normal	One-way ANOVA	1.27E-11	Tukey's	
	Vehicle vs. H_2O_2					8.79E-11
	H_2O_2 vs. H_2O_2+APN					7.58E-01
	Vehicle vs. H_2O_2+APN					8.29E-11
Figure 2B						
Ad-Empty		Normal	One-way ANOVA	4.86E-09	Tukey's	
	Vehicle vs. H_2O_2					4.76E-09
	H_2O_2 vs. H_2O_2+APN					2.67E-03
	Vehicle vs. H_2O_2+APN					2.52E-07
Ad-GRK2		Normal	One-way ANOVA	2.68E-08	Tukey's	
	Vehicle vs. H_2O_2					3.06E-08
	H_2O_2 vs. H_2O_2+APN					1.62E-02
	Vehicle vs. H_2O_2+APN					7.44E-07
Figure 2C						
Ad-Empty		Normal	One-way ANOVA	1.62E-12	Tukey's	

	Vehicle vs. H_2O_2					1.43E-12
	H_2O_2 vs. H_2O_2+APN					3.95E-10
	Vehicle vs. H_2O_2+APN					3.12E-05
Ad-GRK2		Normal	One-way ANOVA	2.94E-08	Tukey's	
	Vehicle vs. H_2O_2					1.32E-07
	H_2O_2 vs. H_2O_2+APN					8.42E-01
	Vehicle vs. H_2O_2+APN					1.32E-07
Figure 2D						
Ad-Empty		Normal	One-way ANOVA	2.14E-09	Tukey's	
	Vehicle vs. H_2O_2					1.37E-09
	H_2O_2 vs. H_2O_2+APN					1.23E-05
	Vehicle vs. H_2O_2+APN					2.62E-06
Ad-GRK2		Normal	One-way ANOVA	3.70E-10	Tukey's	
	Vehicle vs. H_2O_2					2.67E-10
	H_2O_2 vs. H_2O_2+APN					2.68E-05
	Vehicle vs. H_2O_2+APN					1.14E-07
Figure 2G						
Ad-Empty		Normal	One-way ANOVA	2.32E-08	Tukey's	
	Vehicle vs. H_2O_2					1.50E-08
	H_2O_2 vs. H_2O_2+APN					2.03E-05
	Vehicle vs. H_2O_2+APN					7.65E-05
Ad-GRK2		Normal	One-way ANOVA	1.34E-05	Tukey's	
	Vehicle vs. H_2O_2					4.21E-05
	H_2O_2 vs. H_2O_2+APN					7.56E-01
	Vehicle vs. H_2O_2+APN					3.60E-05
Figure 2H						
Ad-Empty		Normal	One-way ANOVA	9.90E-09	Tukey's	
	Vehicle vs. H_2O_2					7.31E-09
	H_2O_2 vs. H_2O_2+APN					2.04E-06
	Vehicle vs. H_2O_2+APN					3.31E-04
Ad-GRK2		Normal	One-way ANOVA	5.66E-08	Tukey's	
	Vehicle vs. H_2O_2					3.62E-08
	H_2O_2 vs. H_2O_2+APN					9.52E-05
	Vehicle vs. H_2O_2+APN					9.52E-05
Figure 3E		Normal	Two-way ANOVA		Tukey's	
	hAdipoR1^{WT}+Ad-Empty vs. hAdipoR1^{WT}+Ad-GRK2					2.16E-08
	hAdipoR1^{S205A}+Ad-Empty vs. hAdipoR1^{S205A}+Ad-GRK2					3.76E-02

	hAdipoR1^{WT}+Ad-GRK2 vs. hAdipoR1^{S205A}+Ad-GRK2					1.48E-05
Figure 3G		Normal	Two-way ANOVA		Tukey's	
	hAdipoR1^{WT}+Ad-Empty vs. hAdipoR1^{WT}+Ad-GRK2					1.33E-08
	hAdipoR1^{S205A}+Ad-Empty vs. hAdipoR1^{S205A}+Ad-GRK2					1.00E+00
	hAdipoR1^{WT}+Ad-GRK2 vs. hAdipoR1^{S205A}+Ad-GRK2					5.01E-09
Figure 4C		Normal	Two-way ANOVA		Tukey's	
	hAdipoR1^{WT}+Ad-Empty vs. hAdipoR1^{WT}+Ad-GRK2					1.27E-09
	hAdipoR1^{S205A}+Ad-Empty vs. hAdipoR1^{S205A}+Ad-GRK2					6.53E-03
	hAdipoR1^{WT}+Ad-GRK2 vs. hAdipoR1^{S205A}+Ad-GRK2					7.19E-06
Figure 4D		Not normal	Kruskal-Wallis	4.23E-04	Dunn's	
	Ad-Empty vs. Ad-GRK2-12h					8.97E-01
	Ad-Empty vs. Ad-GRK2-24h					4.81E-02
	Ad-Empty vs. Ad-GRK2-48h					9.94E-03
	Ad-Empty vs. Ad-GRK2-72h					2.20E-04
Figure 4E		Not normal	Kruskal-Wallis	2.76E-04	Dunn's	
	Ad-Empty+Vehicle vs. Ad-Empty+APN					1.75E-02
	Ad-GRK2+Vehicle vs. Ad-GRK2+APN					1.75E-02
	Ad-Empty+APN vs. Ad-GRK2+APN					5.52E-01
Figure 4F		Not normal	Kruskal-Wallis	1.74E-02	Dunn's	
	Ad-Empty+Vehicle vs. Ad-Empty+APN					1.75E-02
	Ad-GRK2+Vehicle vs. Ad-GRK2+APN					6.56E-01
	Ad-Empty+APN vs. Ad-GRK2+APN					3.13E-02
Figure 4G						
Left		Normal	One-way ANOVA	1.68E-08	Tukey's	
	Ad-GRK2+Vehicle vs. Ad-GRK2+H_2O_2					1.17E-08
	Ad-GRK2+H_2O_2 vs. Ad-GRK2+ H_2O_2+APN					1.05E-03
	Ad-GRK2+Vehicle vs. Ad-GRK2+H_2O_2+APN					5.30E-06
Right		Normal	One-way ANOVA	4.31E-11	Tukey's	
	Ad-GRK2+Vehicle vs. Ad-GRK2+H_2O_2					1.55E-10
	Ad-GRK2+H_2O_2 vs. Ad-GRK2+ H_2O_2+APN					8.71E-01
	Ad-GRK2+Vehicle vs. Ad-GRK2+H_2O_2+APN					2.44E-10
Figure 5A		Not normal	Kruskal-Wallis	8.32E-04	Dunn's	
	Ad-Empty vs. Ad-GRK2-24h					7.97E-01

	Ad-Empty vs. Ad-GRK2-48h					4.81E-02
	Ad-Empty vs. Ad-GRK2-72h					1.98E-03
	Ad-Empty vs. Ad-GRK2-96h					1.09E-03
Figure 5B		Not normal	Kruskal-Wallis	6.47E-01	Dunn's	
	Ad-Empty vs. Ad-GRK2-24h					
	Ad-Empty vs. Ad-GRK2-48h					
	Ad-Empty vs. Ad-GRK2-72h					
	Ad-Empty vs. Ad-GRK2-96h					
Figure 5D						
24h		Not normal	Kruskal-Wallis	7.54E-01	N/A	
	Vehicle vs. MG-132					
	Vehicle vs. Chloroquine					
	MG-132 vs. Chloroquine					
48h		Not normal	Kruskal-Wallis	5.28E-02	N/A	
	Vehicle vs. MG-132					
	Vehicle vs. Chloroquine					
	MG-132 vs. Chloroquine					
72h		Not normal	Kruskal-Wallis	4.67E-03	Dunn's	
	Vehicle vs. MG-132					1.00E+00
	Vehicle vs. Chloroquine					1.55E-02
	MG-132 vs. Chloroquine					1.16E-01
96h		Not normal	Kruskal-Wallis	9.36E-04	Dunn's	
	Vehicle vs. MG-132					1.00E+00
	Vehicle vs. Chloroquine					4.67E-02
	MG-132 vs. Chloroquine					1.73E-02
Figure 6B		Normal	Two-way ANOVA		Tukey's	
	$hAdipoR1^{WT}$+Ad-Empty vs. $hAdipoR1^{WT}$+Ad-GRK2					2.46E-06
	$hAdipoR1^{S205A}$+Ad-Empty vs. $hAdipoR1^{S205A}$+Ad-GRK2					1.14E-03
	$hAdipoR1^{WT}$+Ad-GRK2 vs. $hAdipoR1^{S205A}$+Ad-GRK2					3.74E-02
Figure 6F						
24h		Not normal	Kruskal-Wallis	2.40E-01	N/A	
	$hAdipoR1^{WT}$ vs. $hAdipoR1^{S205A}$					
	$hAdipoR1^{WT}$ vs. $hAdipoR1^{S205E}$					
	$hAdipoR1^{S205A}$ vs. $hAdipoR1^{S205E}$					
48h		Not normal	Kruskal-Wallis	1.75E-02	Dunn's	
	$hAdipoR1^{WT}$ vs. $hAdipoR1^{S205A}$					4.52E-02

	$hAdipoR1^{WT}$ vs. $hAdipoR1^{S205E}$					1.22E-01
	$hAdipoR1^{S205A}$ vs. $hAdipoR1^{S205E}$					1.00E+00
72h		Not normal	Kruskal-Wallis	2.84E-03	Dunn's	
	$hAdipoR1^{WT}$ vs. $hAdipoR1^{S205A}$					2.93E-02
	$hAdipoR1^{WT}$ vs. $hAdipoR1^{S205E}$					5.02E-02
	$hAdipoR1^{S205A}$ vs. $hAdipoR1^{S205E}$					1.00E+00
96h		Not normal	Kruskal-Wallis	3.15E-03	Dunn's	
	$hAdipoR1^{WT}$ vs. $hAdipoR1^{S205A}$					3.85E-02
	$hAdipoR1^{WT}$ vs. $hAdipoR1^{S205E}$					3.85E-02
	$hAdipoR1^{S205A}$ vs. $hAdipoR1^{S205E}$					1.00E+00
Figure 7B		Normal	Two-way ANOVA with a repeated measures ANOVA (based on GLM)		Tukey's	
1 week after MI	Sham vs. MI					3.60E-05
	Sham vs. MI+APN					3.61E-05
	MI vs. MI+APN					8.51E-01
2 weeks after MI	Sham vs. MI					1.44E-05
	Sham vs. MI+APN					2.12E-05
	MI vs. MI+APN					8.87E-01
3 weeks after MI	Sham vs. MI					1.90E-06
	Sham vs. MI+APN					2.61E-06
	MI vs. MI+APN					8.70E-01
4 weeks after MI	Sham vs. MI					7.25E-07
	Sham vs. MI+APN					5.00E-06
	MI vs. MI+APN					5.34E-01
Figure 7C		Normal	Two-way ANOVA with a repeated measures ANOVA (based on GLM)		Tukey's	
1 week after MI	Sham vs. MI					1.84E-05
	Sham vs. MI+APN					1.95E-05
	MI vs. MI+APN					9.99E-01
2 weeks after MI	Sham vs. MI					1.46E-04
	Sham vs. MI+APN					3.28E-04
	MI vs. MI+APN					1.00E+00
3 weeks after MI	Sham vs. MI					1.11E-05
	Sham vs. MI+APN					2.06E-04
	MI vs. MI+APN					8.80E-01
4 weeks after MI	Sham vs. MI					1.06E-04
	Sham vs. MI+APN					5.38E-05
	MI vs. MI+APN					5.19E-01

Figure 7D		Normal	Two-way ANOVA with a repeated measures ANOVA (based on GLM)		Tukey's	
1 week after MI	Sham vs. MI					1.68E-04
	Sham vs. MI+APN					3.68E-05
	MI vs. MI+APN					6.13E-01
2 weeks after MI	Sham vs. MI					3.64E-05
	Sham vs. MI+APN					2.58E-04
	MI vs. MI+APN					9.23E-02
3 weeks after MI	Sham vs. MI					4.89E-07
	Sham vs. MI+APN					4.83E-05
	MI vs. MI+APN					8.08E-03
4 weeks after MI	Sham vs. MI					9.12E-06
	Sham vs. MI+APN					7.14E-04
	MI vs. MI+APN					1.31E-03
Figure 7E		Normal	Two-way ANOVA with a repeated measures ANOVA (based on GLM)		Tukey's	
1 week after MI	Sham vs. MI					2.05E-04
	Sham vs. MI+APN					1.40E-04
	MI vs. MI+APN					9.26E-01
2 weeks after MI	Sham vs. MI					1.48E-04
	Sham vs. MI+APN					1.67E-02
	MI vs. MI+APN					3.67E-01
3 weeks after MI	Sham vs. MI					1.46E-04
	Sham vs. MI+APN					1.31E-02
	MI vs. MI+APN					2.91E-02
4 weeks after MI	Sham vs. MI					2.56E-05
	Sham vs. MI+APN					2.25E-03
	MI vs. MI+APN					1.79E-04
Figure 7H					Tukey's	
Radial Strain		Normal	Two-way ANOVA with a repeated measures ANOVA (based on GLM)			
1 week after MI	Sham vs. MI					1.97E-05
	Sham vs. MI+APN					1.81E-05
	MI vs. MI+APN					8.96E-01
2 weeks after MI	Sham vs. MI					7.01E-06
	Sham vs. MI+APN					1.94E-05
	MI vs. MI+APN					9.53E-01

3 weeks after MI	Sham vs. MI					9.25E-07
	Sham vs. MI+APN					7.16E-07
	MI vs. MI+APN					9.17E-01
4 weeks after MI	Sham vs. MI					3.52E-07
	Sham vs. MI+APN					3.84E-07
	MI vs. MI+APN					6.47E-01
Radial Strain Rate		Normal	Two-way ANOVA with a repeated measures ANOVA (based on GLM)		Tukey's	
1 week after MI	Sham vs. MI					3.75E-03
	Sham vs. MI+APN					3.22E-02
	MI vs. MI+APN					5.00E-01
2 weeks after MI	Sham vs. MI					6.29E-05
	Sham vs. MI+APN					7.37E-05
	MI vs. MI+APN					9.99E-01
3 weeks after MI	Sham vs. MI					8.14E-04
	Sham vs. MI+APN					1.69E-03
	MI vs. MI+APN					7.29E-01
4 weeks after MI	Sham vs. MI					2.22E-03
	Sham vs. MI+APN					4.62E-03
	MI vs. MI+APN					6.91E-01
Longitudinal Strain		Normal	Two-way ANOVA with a repeated measures ANOVA (based on GLM)		Tukey's	
1 week after MI	Sham vs. MI					2.25E-02
	Sham vs. MI+APN					5.49E-03
	MI vs. MI+APN					9.70E-01
2 weeks after MI	Sham vs. MI					9.33E-04
	Sham vs. MI+APN					7.19E-04
	MI vs. MI+APN					9.94E-01
3 weeks after MI	Sham vs. MI					9.46E-05
	Sham vs. MI+APN					1.03E-04
	MI vs. MI+APN					8.95E-01
4 weeks after MI	Sham vs. MI					1.52E-06
	Sham vs. MI+APN					7.04E-05
	MI vs. MI+APN					9.18E-01
Longitudinal Strain Rate		Normal	Two-way ANOVA with a repeated measures ANOVA (based on GLM)		Tukey's	
1 week after MI	Sham vs. MI					5.23E-02

	Sham vs. MI+APN					5.98E-02
	MI vs. MI+APN					9.96E-01
2 weeks after MI	Sham vs. MI					4.08E-03
	Sham vs. MI+APN					4.09E-03
	MI vs. MI+APN					9.19E-01
3 weeks after MI	Sham vs. MI					6.08E-03
	Sham vs. MI+APN					3.55E-03
	MI vs. MI+APN					9.98E-01
4 weeks after MI	Sham vs. MI					5.63E-04
	Sham vs. MI+APN					1.92E-03
	MI vs. MI+APN					8.85E-01
Figure 7I					Tukey's	
Radial Strain		Normal	Two-way ANOVA with a repeated measures ANOVA (based on GLM)			
1 week after MI	Sham vs. MI					6.32E-04
	Sham vs. MI+APN					2.58E-04
	MI vs. MI+APN					9.62E-01
2 weeks after MI	Sham vs. MI					9.29E-05
	Sham vs. MI+APN					7.61E-04
	MI vs. MI+APN					5.11E-02
3 weeks after MI	Sham vs. MI					2.23E-04
	Sham vs. MI+APN					2.56E-03
	MI vs. MI+APN					4.65E-02
4 weeks after MI	Sham vs. MI					6.66E-05
	Sham vs. MI+APN					3.67E-04
	MI vs. MI+APN					1.21E-02
Radial Strain Rate		Normal	Two-way ANOVA with a repeated measures ANOVA (based on GLM)		Tukey's	
1 week after MI	Sham vs. MI					1.98E-02
	Sham vs. MI+APN					4.00E-02
	MI vs. MI+APN					9.57E-01
2 weeks after MI	Sham vs. MI					2.88E-03
	Sham vs. MI+APN					2.90E-02
	MI vs. MI+APN					5.68E-01
3 weeks after MI	Sham vs. MI					3.55E-04
	Sham vs. MI+APN					2.71E-02
	MI vs. MI+APN					4.10E-02
4 weeks after MI	Sham vs. MI					3.07E-04

	Sham vs. MI+APN					2.51E-02
	MI vs. MI+APN					1.16E-02
Longitudinal Strain		Normal	Two-way ANOVA with a repeated measures ANOVA (based on GLM)		Tukey's	
1 week after MI	Sham vs. MI					3.82E-05
	Sham vs. MI+APN					6.66E-06
	MI vs. MI+APN					8.39E-01
2 weeks after MI	Sham vs. MI					2.92E-07
	Sham vs. MI+APN					9.83E-04
	MI vs. MI+APN					7.33E-02
3 weeks after MI	Sham vs. MI					1.93E-06
	Sham vs. MI+APN					1.59E-02
	MI vs. MI+APN					3.50E-02
4 weeks after MI	Sham vs. MI					7.44E-05
	Sham vs. MI+APN					8.13E-03
	MI vs. MI+APN					2.61E-02
Longitudinal Strain Rate		Normal	Two-way ANOVA with a repeated measures ANOVA (based on GLM)		Tukey's	
1 week after MI	Sham vs. MI					7.47E-05
	Sham vs. MI+APN					7.74E-05
	MI vs. MI+APN					1.00E+00
2 weeks after MI	Sham vs. MI					4.93E-04
	Sham vs. MI+APN					2.81E-02
	MI vs. MI+APN					7.75E-02
3 weeks after MI	Sham vs. MI					5.18E-04
	Sham vs. MI+APN					4.74E-02
	MI vs. MI+APN					1.28E-02
4 weeks after MI	Sham vs. MI					4.87E-05
	Sham vs. MI+APN					2.62E-02
	MI vs. MI+APN					3.50E-04
Figure 8B		Normal	Two-way ANOVA with a repeated measures ANOVA (based on GLM)		Tukey's	
	AAV9-hAdipoR1^{WT} Sham vs. AAV9-hAdipoR1^{WT} MI					5.00E-14
	AAV9-hAdipoR1^{WT} Sham vs. AV9-hAdipoR1^{WT} MI+APN					5.00E-14
	AAV9-hAdipoR1^{WT} MI vs. AAV9-hAdipoR1^{WT} MI+APN					3.80E-01

	hAdipoR1^{S205A} Sham vs. AAV9-hAdipoR1^{S205A} MI					5.00E-14
	hAdipoR1^{S205A} Sham vs. AAV9-hAdipoR1^{S205A} MI+APN					6.40E-09
	AAV9-hAdipoR1^{S205A} MI vs. AAV9-hAdipoR1^{S205A} MI+APN					8.93E-09
	AAV9-hAdipoR1^{WT} MI+APN vs. AAV9-hAdipoR1^{S205A} MI+APN					1.48E-11
Figure 8C		Normal	Two-way ANOVA with a repeated measures ANOVA (based on GLM)		Tukey's	
	AAV9-hAdipoR1^{WT} Sham vs. AAV9-hAdipoR1^{WT} MI					2.28E-05
	AAV9-hAdipoR1^{WT} Sham vs. AV9-hAdipoR1^{WT} MI+APN					5.49E-06
	AAV9-hAdipoR1^{WT} MI vs. AAV9-hAdipoR1^{WT} MI+APN					9.98E-01
	hAdipoR1^{S205A} Sham vs. AAV9-hAdipoR1^{S205A} MI					1.25E-04
	hAdipoR1^{S205A} Sham vs. AAV9-hAdipoR1^{S205A} MI+APN					4.07E-01
	AAV9-hAdipoR1^{S205A} MI vs. AAV9-hAdipoR1^{S205A} MI+APN					2.59E-02
	AAV9-hAdipoR1^{WT} MI+APN vs. AAV9-hAdipoR1^{S205A} MI+APN					1.03E-02
Figure 8D		Normal	Two-way ANOVA with a repeated measures ANOVA (based on GLM)		Tukey's	
	AAV9-hAdipoR1^{WT} Sham vs. AAV9-hAdipoR1^{WT} MI					4.93E-04
	AAV9-hAdipoR1^{WT} Sham vs. AV9-hAdipoR1^{WT} MI+APN					3.36E-06
	AAV9-hAdipoR1^{WT} MI vs. AAV9-hAdipoR1^{WT} MI+APN					6.43E-01
	hAdipoR1^{S205A} Sham vs. AAV9-hAdipoR1^{S205A} MI					6.22E-08
	hAdipoR1^{S205A} Sham vs. AAV9-hAdipoR1^{S205A} MI+APN					4.74E-03
	AAV9-hAdipoR1^{S205A} MI vs. AAV9-hAdipoR1^{S205A} MI+APN					1.27E-02
	AAV9-hAdipoR1^{WT} MI+APN vs. AAV9-hAdipoR1^{S205A} MI+APN					1.62E-02
Figure 8E						
Left (p-Ser/GAPDH)		Normal	Two-way ANOVA		Tukey's	
	AAV9-hAdipoR1^{WT} Sham vs. AAV9-hAdipoR1^{WT} MI					6.64E-11
	AAV9-hAdipoR1^{S205A} Sham vs. AAV9-hAdipoR1^{S205A} MI					1.00E+00
	AAV9-hAdipoR1^{S205E} Sham vs. AAV9-hAdipoR1^{S205E} MI					1.00E+00

	AAV9-hAdipoR1^{WT} Sham vs. AAV9-hAdipoR1^{S205E} Sham					1.00E+00
	AAV9-hAdipoR1^{WT} MI vs. AAV9-hAdipoR1^{S205A} MI					8.72E-11
	AAV9-hAdipoR1^{WT} MI vs. hAdipoR1^{S205E} MI					1.22E-10
Right (AdipoR1/GAPDH)		Normal	Two-way ANOVA		Tukey's	
	AAV9-hAdipoR1^{WT} Sham vs. AAV9-hAdipoR1^{WT} MI					2.62E-04
	AAV9-hAdipoR1^{S205A} Sham vs. AAV9-hAdipoR1^{S205A} MI					9.08E-01
	AAV9-hAdipoR1^{S205E} Sham vs. AAV9-hAdipoR1^{S205E} MI					9.99E-01
	AAV9-hAdipoR1^{WT} Sham vs. AAV9-hAdipoR1^{S205E} Sham					2.18E-02
	AAV9-hAdipoR1^{WT} MI vs. AAV9-hAdipoR1^{S205A} MI					8.55E-05
	AAV9-hAdipoR1^{WT} MI vs. hAdipoR1^{S205E} MI					3.66E-01
Figure S3B		Not normal	Kruskal-Wallis	2.70E-05	Dunn's	
	Ad-Empty+Vehicle vs. Ad-Empty+APN					3.60E-02
	Ad-GRK2+Vehicle vs. Ad-GRK2+APN					2.70E-01
	Ad-Empty+APN vs. Ad-GRK2+APN					8.44E-03
Figure S3D		Not normal	Kruskal-Wallis	4.09E-03	Dunn's	
	Ad-Empty+Vehicle vs. Ad-Empty+APN					4.51E-02
	Ad-GRK2+Vehicle vs. Ad-GRK2+APN					1.00E+00
	Ad-Empty+APN vs. Ad-GRK2+APN					2.86E-02
Figure S3F		Not normal	Kruskal-Wallis	1.61E-03	Dunn's	
	Ad-Empty+Vehicle vs. Ad-Empty+APN					4.51E-02
	Ad-GRK2+Vehicle vs. Ad-GRK2+APN					8.25E-01
	Ad-Empty+APN vs. Ad-GRK2+APN					1.78E-02
Figure S5		Not normal	Kruskal-Wallis	1.56E-04	Dunn's	
	Ad-Empty vs. Ad-GRK2-12h					2.83E-01
	Ad-Empty vs. Ad-GRK2-24h					2.55E-02
	Ad-Empty vs. Ad-GRK2-48h					1.48E-03
	Ad-Empty vs. Ad-GRK2-72h					2.10E-05
Figure S6			Log-rank			
	AAV9-hAdipoR1^{WT}-Sham vs. AAV9-hAdipoR1^{WT}-MI					1.20E-02
	AAV9-hAdipoR1^{WT}-MI vs. AAV9-hAdipoR1^{WT}-MI+APN					8.68E-01
	AAV9-hAdipoR1^{WT}-Sham vs. AAV9-hAdipoR1^{WT}-MI+APN					9.50E-03
	AAV9-hAdipoR1^{S205A}-Sham vs. AAV9-hAdipoR1^{S205A}-MI					2.57E-02

	AAV9-hAdipoR1^{S205A}-MI vs. AAV9-hAdipoR1^{S205A}-MI+APN					1.61E-01
	AAV9-hAdipoR1^{S205A}-Sham vs. AAV9-hAdipoR1^{S205A}-MI+APN					1.29E-01
	hAdipoR1^{WT}-MI+APN vs. AAV9-hAdipoR1^{S205A}-MI+APN					3.29E-02
Figure S7						
Left (p-Ser/GAPDH)		Normal		8.85E-03	Tukey's	
	Sham vs. MI					8.98E-03
	Sham vs. MI+Paroxetine					6.94E-01
	MI vs. MI+Paroxetine					4.53E-02
Right (AdipoR1/GAPDH)		Normal		3.50E-05	Tukey's	
	Sham vs. MI					2.28E-05
	Sham vs. MI+Paroxetine					1.01E-02
	MI vs. MI+Paroxetine					1.52E-02